Published in final edited form as:
Neurotoxicology. 2006 September ; 27(5): 737–744. doi:10.1016/j.neuro.2006.02.003.

Molecular mechanism of distorted iron regulation in the blood–CSF barrier and regional blood–brain barrier following in vivo subchronic manganese exposure

G. Jane Li[a], **Byung-Sun Choi**[a], **Xueqian Wang**[a], **Jie Liu**[b], **Michael P. Waalkes**[b], and **Wei Zheng**[a,*]

[a]School of Health Sciences, Purdue University, 550 Stadium Mall Drive, CIVL 1163D, West Lafayette, IN 47907, USA

[b]Center for Cancer Research, Inorganic Carcinogenesis Section, NCI at NIEHS, Research Triangle Park, NC 27709, USA

Abstract

Previous studies in this laboratory indicated that manganese (Mn) exposure in vitro increases the expression of transferrin receptor (TfR) by enhancing the binding of iron regulatory proteins (IRPs) to iron responsive element-containing RNA. The current study further tested the hypothesis that in vivo exposure to Mn increased TfR expression at both blood–brain barrier (BBB) and blood–cerebrospinal fluid (CSF) barrier (BCB), which contributes to altered iron (Fe) homeostasis in the CSF. Groups of rats (10–11 each) received oral gavages at doses of 5 mg Mn/kg or 15 mg Mn/kg as $MnCl_2$ once daily for 30 days. Blood, CSF, and choroid plexus were collected and brain capillary fractions were separated from the regional parenchyma. Metal analyses showed that oral Mn exposure decreased concentrations of Fe in serum (−66%) but increased Fe in the CSF (+167%). Gel shift assay showed that Mn caused a dose-dependent increase of binding of IRP1 to iron responsive element-containing RNA in BCB in the choroid plexus (+70%), in regional BBB of capillaries of striatum (+39%), hippocampus (+56%), frontal cortex (+49%), and in brain parenchyma of striatum (+67%), hippocampus (+39%) and cerebellum (+28%). Real-time RT-PCR demonstrated that Mn exposure significantly increased the expression of TfR mRNA in choroid plexus and striatum with concomitant reduction in the expression of ferritin (Ft) mRNA. Collectively, these data indicate that in vivo Mn exposure results in Fe redistribution in body fluids through regulating the expression of TfR and ferritin at BCB and selected regional BBB. The disrupted Fe transport by brain barriers may underlie the distorted Fe homeostasis in the CSF.

Keywords

Manganese (Mn); Iron (Fe); Brain-Barrier system; Iron regulatory protein (IRP); Iron responsive element (IRE); Transferrin receptor (TfR); Oral administration; Choroid plexus (CP); Blood; CSF barrier (BCB); Blood; brain barrier; Ferritin (Ft)

1. Introduction

Manganese (Mn) exposure induces clinical symptoms resembling the Parkinson's disease (Barbeau, 1985; Gorell et al., 1997; Tepper, 1961). The sources of exposure to Mn are numerous but the most significant contributors are occupational and environmental exposure

*Corresponding author at: Tel.: +1 765 496 6447; fax: +1 765 496 1377. wzheng@purdue.edu (W. Zheng).

including inhalation and ingestion. The respiratory and gastrointestinal (GI) tracts are the main portals of entry of Mn in humans. Consumption of drinking water contaminated with Mn has been found to be associated with neurological signs of chronic Mn poisoning (Kondakis et al., 1989; WHO, 1981). However, the mechanism of Mn-induced Parkinsonism has not been completely elucidated.

Earlier studies of Aschner's group (Aschner and Aschner, 1990; Aschner et al., 1999) suggest that iron (Fe) homeostasis may play an important role in the regulation of Mn transport across the blood–brain barrier (BBB). Evidence from this laboratory further indicates that Mn toxicity appears to be associated with altered Fe metabolism at both systemic and cellular levels (Li et al., 2004, 2005; Zheng et al., 1999; Zheng and Zhao, 2001). In vivo Mn exposure via intraperitoneal (i.p.) injection expedites unidirectional influx of Fe from the systemic circulation to cerebral compartment (Zheng et al., 1999); in vitro Mn exposure in a choroidal epithelial Z310 cell line also shows an increased flux of Fe across the blood–cerebrospinal fluid (CSF) barrier (BCB) in an in vitro BCB barrier model (Li et al., 2005), all of which support the view that Mn neurotoxicity is associated with a compartment shift of Fe from the blood circulation to the CSF. The interaction of Mn on Fe homeostasis has also been demonstrated among welders who were occupationally exposed to Mn in welding fume (Crossgrove and Zheng, 2004; Li et al., 2004; Lu et al., 2005).

Our previous work indicates that the mimicry between Mn and Fe in their coordination chemistry allows Mn to compete with Fe in the fourth, labile Fe binding site in the active center of iron regulatory proteins (IRPs), alter the expression of Fe uptake-related protein transferrin receptor (TfR), and increase the cellular overload of Fe at the BCB (Li et al., 2005; Zheng et al., 1998; Zheng, 2001). In an in situ brain perfusion model, we have shown that the transport of Tf-bound Fe and free Fe into the CNS is determined by the initial sequestration by the choroid plexus and brain capillaries, and subsequent controlled and slow release from vascular structures into brain interstitial fluid and CSF (Deane et al., 2004). Thus, a distorted regulation of TfR and ferritin (Ft) expression by toxic substances is expectedly to alter Fe transport at both BBB and BCB since both of TfR and ferritin (Ft) are present at brain barriers (Deane et al., 2004; Li and Qian, 2002). Recent study in our group further explored that Mn exposure in vitro increases the expression of TfR mRNA by enhancing the binding of IRPs to RNA which contains iron responsive element (IRE) stem-loop structure and results in alteration of Fe distribution in the immortalized Z310 epithelial cells (Li et al., 2005). However, little is known about whether this scenario would occur in vivo following oral Mn exposure for a relative long period. Verification of this novel observation of Mn interaction with IRPs in intact animals will help understand the important mechanism by which Fe is regulated at BCB and BBB and how Mn may alter these processes.

The current study was designed to use subchronic oral Mn exposure model to test the hypothesis that in vivo exposure to Mn distorted TfR expression at brain barriers, which contributed to an altered Fe homeostasis in the CSF. Experiments were performed to determine Fe status in serum, CSF, choroid plexus, and selected brain regions following sub-chronic Mn exposure, to determine the effect of oral Mn exposure on the binding activity of IRP1 to IRE-RNA at BCB in the choroid plexus, regional BBB capillaries, and regional brain parenchyma, and to determine cellular mRNA levels of TfR and ferritin in these selected brain regions as affected by in vivo Mn exposure.

2. Materials and methods

2.1. Materials

Chemicals were obtained from the following sources: standard Mn and Fe for atomic absorption spectrophotometry (AAS) from Perkin-Elmer Instruments (Shelton, CT); nitric acid (69.9%, Ultrapure) from J.T. Baker (Phillipsburg, NJ); RNase-free DNase I from Invitrogen Life Technologies (Carlsbad, CA); ATP, GTP, CTP, and UTP (NTPs), [α-^{32}P]UTP from Amersham (Piscataway, NJ); manganese chloride ($MnCl_2 \cdot 4H_2O$), dextran, and all other chemicals from Sigma Chemicals (St. Louis, MO). All reagents were of analytical grade, HPLC grade or the best available pharmaceutical grade.

2.2. Animals

Male Sprague–Dawley rats were purchased from Harlan Sprague–Dawley Inc., Indianapolis, IN. At the time of use the rats were 7–8 weeks old weighing 239 ± 1.8 g (mean ± S.E.M.). Upon arrival, the rats were housed in a temperature-controlled, 12/12 light/dark room, and acclimated for 1 week prior to experimentation. They were allowed to have free access to chaw Laboratory Rodent Diet 5001 PMI (aka Purina Mills, Inc.) and tap water. The study was conducted in complying with animal rights and approved by Institutional Committee on Animal Uses at Purdue University.

2.3. Mn administration and sample collection

$MnCl_2$ dissolved in sterile saline was administered to rats by oral gavage at a dose of 5 or 15 mg of Mn/kg once daily between 9:00 a.m. and 10:00 a.m. for 30 consecutive days except for weekends. This dose regimen was chosen based on our own previous Mn neurotoxicity studies in humans as well in animals (Crossgrove and Zheng, 2004; Zheng et al., 1998, 2000). For the control group, the animals received the daily oral gavage of the equivalent volume of sterile saline. Twenty-four hour after the last oral gavage, rats were anesthetized with pentobarbital (50 mg/kg, i.p.). CSF samples were obtained through a 26-gauge needle inserted between the protruberance and the spine of the atlas, and were free of the blood (Zheng et al., 1991). Blood samples were collected from the inferior vena cava into syringes. Following standing in room temperature for at least half an hour, the blood was centrifuged at 3400 rpm for 30 min and the serum was transferred to an Eppendorf tube. Both CSF and serum samples were stored at −20 °C until analyzed. Rat brains were dissected from the skull and the choroid plexus collected from lateral and third ventricles. Various brain regions, i.e., striatum (ST), hippocampus (HC), frontal cortex (FC), and cerebellum (CB), were dissected. The capillary fractions from these regions were separated from parenchyma by our method previously reported (Deane et al., 2004) and frozen at −70 °C for further isolation of total RNA and S100 extractions.

2.4. Atomic absorption spectrophotometry (AAS) analysis

Mn and Fe concentrations in the CSF and plasma were determined by an HGA-800 graphite furnace AAS system (Perkin-Elmer Instruments, Norwalk, CT) equipped with a Perkin-Elmer Analyst 100 atomic absorption spectrophotometer. Aliquots (50 μL) of CSF and serum were diluted by 50 μL of distilled, deionized water prior to AAS for Mn measurement and diluted 50-fold for Fe measurement. The detection limit of these methods was 0.5 ng/mL of assay solution for Mn and 0.05 μg/dL for Fe.

2.5. Gel shift assay

A gel shift assay was conducted to determine the interaction between IRP1 and mRNA containing IRE as described previously (Li et al., 2005; Lin et al., 2001). The procedure consisted of three major steps. (1) *Extraction of S100 cytoplasmic protein:* choroid plexus,

as well as capillary and parenchyma from various brain regions with or without Mn exposure were homogenized, followed by centrifugation at 100,000 × *g* for 1 h. The supernatant was dialyzed for 8 h against 20 volumes of degassed dialysis buffer composed of 20 mM HEPES, 0.1 M KCl, 20% (v/v) glycerol, 0.2 mM EDTA, 0.5 mM PMSF, and 0.5 mM dithiothreitol (DTT) using Spectra/Pro 96-well MicroDialyzer (150 μL capacity, Spectrum Laboratories, Rancho Dominguez, CA). The S100 cytoplasmic extracts were stored at −80 °C until use.

(2) *Preparation of RNAs containing stem-loop structure:* the DNA oligonucleotide template T7-1 (sequence: 5′-TAA TAC GAC TCA CTA TA-3′) was annealed to ferritin-IRE (Ft-IRE, 2 μM) (sequence: 5′-GGA TCC GTC CAA GCA CTG TTG AAG CAG GAT CCT CTC CCT ATA GTG AGT CGT ATTA) (customer synthesized by IDT, Coralville, IA) in 50 μL anneal buffer (10 mM Tris–HCl pH 7.5 and 10 mM $MgCl_2$). The mixture was heated to and maintained at 95 °C for 5 min and then cooled to less than 35 °C before operating the next step. The transcription reaction was carried out in a total of 50 μL with 0.2 μM annealed template, 12.5 U T7 RNA polymerase, 2 mM each of ATP, GTP, and CTP, 30 μM UTP, and 0.33 μM [α-^{32}P]UTP for 3.5 h at 37 °C, followed by RNA precipitation. The labeled RNA was further purified on a 15% denatured polyacrylamide gel. The bands corresponding to transcription products were excised and eluted; the RNA was recovered, precipitated, and then resuspended in water to at least 10,000 cpm/μL. The products of RNAs containing Ft stem-loop structure were frozen at −80 °C until use (Lin et al., 2001).

(3) *Gel shift assay:* the S100 cytoplasmic extracts (30 μg of protein) were incubated with an excess (0.2 ng, 10^5 cpm) of [^{32}P]-labeled IRE-containing RNA in a gel shift buffer (10 mM HEPES, pH 7.6, 3 mM $MgCl_2$, 40 mM KCl, 5% glycerol, and 1 mM DTT) at 20 °C for 30 min (Leibold and Munro, 1988). One unit of RNase T1 and 5 mg/mL heparin were added to destroy the unprotected RNA and to minimize nonspecific protein–RNA interaction. The mixtures were then loaded on 4% non-denature polyacrylamide gels and visualized by autoradiography. The intensity of protein-RNA bound bands was quantified using UN-SCAN-IT™ (version 5.1) software (Silk Scientific Inc., Orem, Utah).

2.6. Quantitative real-time RT-PCR analysis of TfR and Ft mRNA

Levels of TfR and Ft (heavy chain and light chain) mRNA were quantified using real-time RT-PCR analysis as described by Walker (2001) and Liu et al. (2004a, 2004b). Briefly, total RNA was isolated from choroid plexus, capillary and parenchyma from various brain regions using TRIzol reagent (Invitrogen, Carlsbad, CA), followed by purification on RNeasy columns (Qiagen, Palo Alto, CA). Purified 1 μg of RNA was reverse transcribed with MuLV reverse transcriptase (Applied Biosystems, Foster City, CA) and oligo-dT primers. The forward and reverse primers for GAPDH and target genes were designed using Primer Express 2.0 software (Applied Biosystems, Foster City, CA). The ABsolute QPCR SYBR green Mix kit (ABgene, Rochester, NY) was used for real-time PCR analysis. The amplification was carried out in the Mx3000P Real-Time PCR System (Stratagene, La Jolla, CA). Amplification conditions were 15 min at 95 °C, followed by 40 cycles of 30 s at 95 °C, 1 min at 60 °C, and 30 s at 72 °C, following a dissociation curve at the end of the run to ensure that the primers produce a single clean product. The dissociation program was summarized as below: incubate the amplified product for 1 min at 95 °C, ramping down to 55 °C at a rate of 0.2 °C/s, then complete 81 cycles of incubation where the temperature was increased by 0.5 °C/cycle, beginning at 55 °C and ending at 95 °C. The duration of each cycle was set to 30 s.

Primers sequences used for real-time RT-PCR analysis were: for rat TfR using a forward primer 5′-CTA GTATCT TGA GGT GGG AGG AAG AG-3′ and reverse primer 5′-GAG AAT CCC AGT GAG GGT CAG A-3′ (Genbank Accession No. M58040), for rat Ft light

chain using a forward primer 5′-GTG AAC CGC CTG GTC AAC TT-3′ and reverse primer 5′-AAC CCG AGC TAC TCA CCA GAG A-3′ (Genbank Accession No. J02741), for rat Ft heavy chain using a forward primer 5′-CAA GTG CGC CAG AAC TAC CA-3′ and reverse primer 5′-GTG TCC CAG GGT GTG CTT GT-3′ (Genbank Accession No. M18051); for rat glyceraldehyde-3-phosphate dehydrogenase (GAPDH), used as an internal control, using a forward primer 5′-CCT GGA GAA ACC TGC CAA GTA T-3′ and reverse primer 5′-AGC CCA GGA TGC CCT TTA GT-3′ (Genbank Accession No. NM017008).

The relative differences in gene expression between groups were expressed using cycle time values; the values of these interested genes were first normalized with that of GAPDH in the same sample, and then the relative differences between control and treatment groups were calculated and expressed as relative increases by setting the control as 100%. Assuming that the value is reflective of the initial starting copy and that there is 100% efficiency, a difference of one cycle is equivalent to a two-fold difference in starting copy (Liu et al., 2004a, 2004b; Walker, 2001).

2.7. Statistical analysis

All data are expressed as mean ± S.E.M. and analyzed by SPSS 11.5 statistic package for Windows. The replicates of experiments conducted in the same day were referred as $n = 1$; three to six such replicates on different dates were used for statistical analyses. The statistical analyses were carried out by analysis of variance (ANOVA) using post hoc test on Mn-treated groups and controls with a significance level at $p < 0.05$. More specifically, we select LSD and Duncan tests for the “Equal Variance Assumed” test and select Tamhane’s T2 for “Equal Variance Not Assumed” test.

3. Results

3.1. Concentrations of Mn and Fe in body fluids and brain regions following in vivo Mn exposure

Subchronic oral exposure to Mn in the rats at the dose of 5 (low dose) and 15 (high dose) mg/kg/day through oral gavage for 30 days resulted in a logarithmic dose-dependent increase of Mn in serum ($r = 0.463$, $p = 0.030$), but not in the CSF ($r = 0.292$, $p = 0.257$. Fig. 1).

Subchronic oral exposure to Mn resulted in a Mn dose-dependent decrease of serum Fe concentration. Serum Fe concentration was declined by 50% and 66% of controls at the low and high dose levels, respectively ($p < 0.01$, Fig. 2). In contrast, the Fe concentration in the CSF increased dramatically by 136% and 167% compared to the controls at the low ($p < 0.05$) and high dose ($p < 0.01$, Fig. 2). The ratio of CSF to serum Fe ($Fe_{CSF/serum}$) was increased from 0.05 in control rats to 0.24 and 0.43 in the low and high doses, respectively, reflecting an elevated Fe in the CSF compartment, which is comparable to our previous observation (Zheng et al., 1999).

3.2. Increased binding of IRP1 to IRE-contained RNAs in BCB, selected regional BBB, and brain parenchyma following in vivo Mn exposure

The S100 cytosolic extracts from brain samples were used for the gel shift assay to study binding of IRP1 to in vitro transcripted ^{32}P-labeled IRE containing RNA probes. Following subchronic in vivo Mn exposure, the shifted bands representing the binding of IRP1 to IRE stem-loop RNA were visibly increased in the CP, capillary fractions and parenchyma of Mn-treated animals as compared to controls (Fig. 3A). It is noticed that the IRP1-RNA complexes from choroid plexus tissues were not located at the exact position between

control and Mn-treated groups. This could be due to experimental variations when the gel was heated under high voltage.

Further analyses by densitometry revealed a statistically significant 70% increase of binding above the controls in the choroid plexus at the high dose group. Among cerebral capillaries determined, there were 39% increase in striatum at the high dose, 45–56% increase in hippocampus at both Mn doses, and 49% increase in frontal cortex at the high dose, but no change in cerebellum. Mn exposure at the high dose also potentiated the binding of IRP1 to IRE-RNA in brain parenchyma of striatum (67% increase above the controls), hippocampus (39% increase), and cerebellum (28% increase), but not in parenchyma of the frontal cortex (Fig. 3B).

3.3. Increased expression of TfR mRNA and decreased expression of Ft mRNAs in BCB, selected regional BBB, and brain parenchyma following in vivo Mn exposure

Quantitative real-time RT-PCR was used to quantify the effect of subchronic oral Mn exposure on the levels of TfR. The results indicated that Mn treatment significantly increased the amount of TfR mRNA in the choroid plexus by 69% above the controls at the low dose group (Fig. 4A). Most striking effect was observed in striatum, where 125% and 90% increases above controls were observed in striatal capillary and parenchyma, respectively, in the high dose groups. Mn treatment did not affect TfR mRNA levels in capillaries of frontal cortex and cerebellum, nor did it affect TfR mRNA expression in parenchyma of these regions at all studied doses.

Quantitative real-time RT-PCR was also used to study the levels of Ft mRNA. Cellular Ft exists in two isoforms, i.e., heavy-chain ferritin, Ft(H) and light-chain ferritin, Ft(L). Mn exposure induced a significant decrease in the amount of Ft(H) in the choroid plexus by 87% less than that of controls; it also decreased Ft(H) mRNA levels by 34% and 46% less than those of controls in striatal capillary and parenchyma, respectively (Fig. 4B). Neither in capillary nor parenchyma Ft(H) mRNA was affected by Mn treatment in hippocampus, frontal cortex as well as cerebellum.

Mn exposure had no statistically significant effect on the levels of Ft(L) mRNA in all tested regions except for the choroid plexus ($p < 0.05$, Fig. 4C).

4. Discussion

The results of this study clearly demonstrate that subchronic oral exposure to Mn decreases serum Fe concentrations while it increases the Fe concentration in the CSF. The altered Fe homeostasis in body fluids appears to be associated with an increased binding of IRP1 to IRE stem-loop-contained RNA and the ensuing up-regulation of TfR at brain barriers. Fe is an essential element for normal brain development and function. However, excess accumulation of Fe in cells promotes oxidative injury (Halliwell and Gutteridge, 1990). Abnormal Fe homeostasis, both systemically and subcellularly, is believed to be associated with etiology of idiopathic Parkinson's disease and chemical-induced Parkinsonism (Jenner, 2003; Loeffler et al., 1995; Yantiri and Andersen, 1999; Youdim, 2003), such as Mn-induced Parkinsonism (Crossgrove and Zheng, 2004; Zheng et al., 2003). The present study clearly demonstrated that oral Mn exposure significantly altered Fe homeostasis in the blood and the CSF. The current observation of a significant decrease of Fe concentrations in serum accompanying with an increase of Fe in the CSF is consistent with our previous results from the intraperitoneal (i.p.) dose study (Zheng et al., 1999). The ratio of CSF to serum Fe ($Fe_{CSF/serum}$), an index reflecting Fe distribution in two fluid compartments (Nazifi and Maleki, 1998; Zheng et al., 1999), was increased from 0.05 in control rats to 0.43 in the Mn-treated rats in present study, a nearly ninefold increase that reflects an influx of Fe from the

systemic circulation to the cerebral compartment following oral Mn exposure, indicating that brain Fe homeostasis appeared to be susceptible to Mn exposure.

It should also be noted that the deposition of oral Mn is quite different from Mn intoxication by non-oral routes. Our previous studies with i.p. injections of $MnCl_2$ for 30 days show a 10-fold increase in plasma Mn levels and 11-fold increase in CSF Mn concentration (Zheng et al., 1999). While the current data displayed a trend of increase in Mn concentrations in both serum (60%) and CSF (40%) following $MnCl_2$ oral exposure at 15 mg Mn/kg/day for 30 days, the linear correlation between dose and CSF Mn was not statistically significant. This discrepancy is largely due to the different routes of Mn dose administration. Mn has a relatively short blood half life ($t_{1/2} < 2$ h) and large volume of distribution, disappearing rapidly from the blood compartment. The absolute bioavailability was less than 15% after oral administration of $MnCl_2$ (Zheng et al., 2000). Our current study with an upward dose–response curve, yet insignificant change of CSF Mn at day 30 may reflect the poor bioavailability and rapid clearance of this metal following oral dose. Other studies by oral dose of Mn show the similar characteristics of kinetics. For example, Roels and colleagues (1997) administered a single oral dose of $MnCl_2$ (24.3 mg Mn/kg b.w.) and observed a transient rise in blood Mn concentrations, which were about five times lower than those with Mn by the intra-tracheal (i.t.) instillation. A peak value of 1.66 μg Mn/dL was reached after 1 h of dosing following by a rapid return to control values within 12 h. These authors conclude that the pattern of the time course of blood Mn most likely reflects a limited transfer of Mn from the GI tract into the circulation after oral administration.

The transfer of a substance from the blood into the brain occurs either at the cerebral vasculature and/or via the CSF (Bradbury, 1979). Uptake into cerebral cortex mainly results from transport at the cerebral capillary endothelium, whereas uptake into the ventricular CSF is associated with transport across the choroid plexus during short circulation times (Smith and Rapoport, 1986). This study for the first time demonstrated that Mn-induced RNA–protein interaction between IRP1 and IRE-RNA coincided with increased TfR mRNA levels in the same brain regions. These observations suggest that proteins involving in Fe metabolic regulation seem likely to be highly susceptible to intracellular fluctuation of Mn concentrations along with other factors such as altered Fe levels or increased oxidative stress. Considering the low dose and long-term environmental/occupational exposure to Mn in real life, the subchronic oral Mn exposure model in the present study appears to be more relevant to human exposures than i.p. Mn exposure models.

The mechanism by which Mn alters brain Fe homeostasis is a major focus of the present study. Under normal physiological conditions, brain Fe homeostasis is mainly regulated by TfR and Ft. TfR is a membrane glycoprotein whose only clearly defined function is to mediate cellular uptake of Fe from Fe carrying glycoprotein, Tf (Ponka and Lok, 1999). Fe molecules, upon taken up by the brain barrier cells, are stored intracellularly in Ft, which contains 24 subunits, made of heavy (H) and light (L) polypeptide chains that are encoded by different genes (Lawson et al., 1991; Munro, 1993). The H-chain is responsible for the rapid oxidation, storage, and uptake of Fe (Cozzi et al., 2000). It acts as a regulator of the cellular labile Fe pool and as an attenuator of the cellular oxidative response (Epsztejn et al., 1999; Geiser et al., 2003). The L-chain, on the other hand, creates a nucleation site for Fe and is essential for formation of the Fe core, which is a complex of Fe, phosphate and oxygen (Munro, 1993; Ponka et al., 1998). The cellular abundance of TfR and Ft is regulated by IRPs whose [4Fe-4S] configuration changes in response to cell's need for labile Fe. The regulation of Ft expression is thought to occur at translational level by binding and unbinding of IRPs to IRE stem loop contained RNAs (Ponka and Lok, 1999). Our results from gel shift assay clearly demonstrated that in vivo Mn exposure remarkably increased the binding of IRP1 to IRE-contained RNA in BCB and selected regional BBB, particularly in

striatum. Moreover, the increased protein–RNA interaction appeared to lead to an elevated TfR mRNA in these regions by quantitative real-time RT-PCR assay. Since the IRE stem loops in TfR mRNA are located in 3′-UTR, the binding of IRPs to the IRE is likely to stabilize the TfR mRNA and thus reduce the degradation of TfR mRNA. Noticeably also, the IRE stem loop is located at 5′-UTR of Ft mRNA, with which the binding of IRPs would repress the translational expression of Ft protein. The current results that in vivo Mn exposure caused a decrease of Ft mRNA in BCB and in striatum capillaries further support the aforementioned hypothesis. Thus, an up-regulated membrane surface TfR and down-regulated Fe storage Ft at the BCB, as we observed here, would seem likely to underlie the compartmental shift of Fe from the blood to the CSF following subchronic Mn exposure in vivo.

Our observation of Mn alteration of Fe homeostasis from this and earlier studies (Li et al., 2005; Zheng et al., 1999) raises several interesting questions: how does the brain protect itself from the escalating influx of Fe? Is the elevated Fe concentration in the CSF a protective means to remove the excess Fe in the cerebral compartment? By what mechanism do the BBB and BCB act in concert to deal with the elevated Fe in the CSF? Is Mn effect on CSF Fe associated with systemic Fe dysregulation within the context of overall Fe homeostasis that is regulated by liver, macrophages, and other means? At present, there is no satisfactory answer to any of these questions. Future research directed toward these unsolved questions would not only help understand the mechanism of Mn action at the brain barriers, but also better recognize the physiology and pathophysiology of Fe regulation by the brain barriers under normal and disease status.

In summary, the present work indicates that in vivo Mn exposure by oral administration increased the binding of IRP1 to IRE-containing RNAs encoding Ft in the BCB and selected regional BBB, particularly in striatum, as well as in brain parenchyma. The ensuing increase in the expression of TfR and decrease in Ft in those brain regions may facilitate the influx of Fe into the brain compartment. Interference of Fe transport by Mn may contribute to Mn-induced neurotoxicity.

Acknowledgments

The authors wish to acknowledge the assistance of Maneesha Chigurupati for sample preparation. This project was supported by NIH/National Institute of Environmental Health Sciences Grant ES-08146 (WZ) and partly by the Intramural Research Program of the NIH, National Cancer Institute, Center for Cancer Research (JL and MW).

References

Aschner M, Aschner JL. Mn transport across the blood–brain barrier: relationship to Fe homeostasis. Brain Res Bull. 1990; 24:857–60. [PubMed: 2372703]

Aschner M, Vrana KE, Zheng W. Mn uptake and distribution in the central nervous system (CNS). Neurotoxicology. 1999; 20:173–80. [PubMed: 10385881]

Barbeau A. Mn and extrapyramidal disorders. Neurotoxicology. 1985; 5:13–6. [PubMed: 6538948]

Bradbury, M. The concept of a blood–brain barrier. Chichester, UK: John Wiley; 1979.

Cozzi A, Corsi B, Levi S, Santambrogio P, Albertini A, Arosio P. Over-expression of wild type and mutated human ferritin H-chain in HeLa cells: in vivo role of ferritin ferroxidase activity. J Biol Chem. 2000; 275:25122–9. [PubMed: 10833524]

Crossgrove J, Zheng W. Mn toxicity upon overexposure. NMR Biomed. 2004; 17:544–53. [PubMed: 15617053]

Deane R, Zheng W, Zlokovic BV. Brain capillary endothelium and choroid plexus epithelium regulate transport of transferrin-bound and free Fe into the rat brain. J Neurochem. 2004; 88:813–20. [PubMed: 14756801]

Epsztejn S, Glickstein H, Picard V, Slotki IN, Breuer W, Beaumont C, et al. H-ferritin subunit overexpression in erythroid cells reduces the oxidative stress response and induces multidrug resistance properties. Blood. 1999; 94:3593–603. [PubMed: 10552971]

Geiser DL, Chavez CA, Flores-Munguia R, Winzerling JJ, Pham DQ. Aedes aegypti ferritin. Eur J Biochem. 2003; 270:3667–74. [PubMed: 12950250]

Gorell JM, Johnson CC, Rybicki BA, Peterson EL, Kortsha GX, Brown GG, et al. Occupational exposures to metals as risk factors for Parkinson's disease. Neurology. 1997; 48:650–8. [PubMed: 9065542]

Halliwell B, Gutteridge JM. Role of free radicals and catalytic metal ions in human disease: an overview. Methods Enzymol. 1990; 186:1–85. [PubMed: 2172697]

Jenner P. Oxidative stress in Parkinson's disease. Ann Neurol. 2003; 53(Suppl 3):S26–36. discussion S36–38. [PubMed: 12666096]

Kondakis XG, Makris N, Leotsinidis M, Prinou M, Papapetropoulos T. Possible health effects of high Mn concentration in drinking water. Arch Environ Health. 1989; 44:175–8. [PubMed: 2751354]

Lawson DM, Artymiuk PJ, Yewdall SJ, Smith JMA, Livingstone JC, Treffry A, et al. Solving the structure of human H ferritin by genetically engineering intermolecular crystal contacts. Nature. 1991; 349:541–4. [PubMed: 1992356]

Leibold EA, Munro HN. Cytoplasmic protein binds in vitro to a highly consered sequence in the 5′ untranslated region of ferritin heavy- and light-subunit mRNAs. Proc Natl Acad Sci USA. 1988; 85:2171–5. [PubMed: 3127826]

Li GJ, Zhang LL, Lu L, Wu P, Zheng W. Occupational exposure to welding fume among welders: alterations of Mn, Fe, zinc, copper, and lead in body fluids and the oxidative stress status. J Occup Environ Med. 2004; 46:241–8. [PubMed: 15091287]

Li GJ, Zhao Q, Zheng W. Alteration at translational but not transcriptional level of transferrin receptor expression following Mn exposure at the blood–CSF barrier in vitro. Toxicol Appl Pharmacol. 2005; 205:188–200. [PubMed: 15893546]

Li H, Qian ZM. Transferrin/transferrin receptor-mediated drug delivery. Med Res Rev. 2002; 22:225–50. [PubMed: 11933019]

Lin E, Graziano JH, Freyer GA. Regulation of the 75 kDa subunit of mitochondrial complex I by iron. J Biol Chem. 2001; 276:27685–92. [PubMed: 11313346]

Liu J, Xie Y, Ward JM, Diwan BA, Waalkes MP. Toxicogenomic analysis of aberrant gene expression in liver tumors and nontumorous livers of adult mice exposed in utero to inorganic arsenic. Toxicol Sci. 2004a; 77:249–57. [PubMed: 14691202]

Liu J, Walker N, Waalkes MP. Hybridization buffer systems impact the quality of filter array data. J Pharmacol Toxicol Methods. 2004b; 50:67–71. [PubMed: 15233970]

Loeffler DA, Connor JR, Juneau PL, Snyder BS, Kanaley L, DeMaggio AJ, et al. Fe in normal, Alzheimer's disease, and Parkinson's disease brain regions. J Neurochem. 1995; 65:710–24. [PubMed: 7616227]

Lu L, Zhang LL, Li GJ, Guo WR, Liang WN, Zheng W. Alteration of serum concentrations of Mn, Fe, ferritin, and transferrin receptor following exposure to welding fumes among career welders. Neurol Toxicol. 2005; 26:257–65.

Munro H. The ferritin genes: their response to Fe status. Nutr Rev. 1993; 51:65–73. [PubMed: 8502427]

Nazifi S, Maleki K. Biochemical analysis of serum and cerebrospinal fluid in clinically normal adult camels (*Camelus dromedaries*). Res Vet Sci. 1998; 65:83–4. [PubMed: 9769078]

Ponka P, Beaumont C, Richardson DR. Function and regulation of transferrin and ferritin. Semin Hematol. 1998; 35:35–54. [PubMed: 9460808]

Ponka P, Lok CN. The transferrin receptor: role in health and disease. Int J Biochem Cell Biol. 1999; 31:1111–37. [PubMed: 10582342]

Roels H, Meiers G, Delos M, Ortega I, Lauwerys R, Buchet JP, et al. Influence of the route of administration and the chemical form ($MnCl_2$, MnO_2) on the absorption and cerebral distribution of Mn in rats. Arch Toxicol. 1997; 71:223–30. [PubMed: 9101038]

Smith QR, Rapoport SI. Cerebrovascular permeability coefficients to sodium, potassium, and chloride. J Neurochem. 1986; 46:1732–42. [PubMed: 3084708]

Tepper LB. Hazards to health: Mn. N Engl J Med. 1961; 264:347–8. [PubMed: 13775934]

Walker NJ. Real-time and quantitative PCR: applications to mechanism-based toxicology. J Biochem Mol Toxicol. 2001; 15:121–7. [PubMed: 11424221]

WHO. Environmental health criteria 17. Manganese. Geneva: World Health Organization; 1981.

Yantiri F, Andersen JK. The role of Fe in Parkinson disease and 1-methyl-4-phenyl-1,2,3,6-tetrahydropyridine toxicity. IUBMB Life. 1999; 48:139–41. [PubMed: 10794588]

Youdim MB. What have we learnt from CDNA microarray gene expression studies about the role of Fe in MPTP induced neurodegeneration and Parkinson's disease? J Neural Transm Suppl. 2003; 65:73–88. [PubMed: 12946050]

Zheng W. Neurotoxicology of the brain barrier system: new implications. J Toxicol Clin Toxicol. 2001; 39:711–9. [PubMed: 11778669]

Zheng W, Perry DF, Nelson DL, Aposhian HV. Protection of cerebrospinal fluid against toxic metals by the choroid plexus. FASEB J. 1991; 5:2188–93. [PubMed: 1850706]

Zheng W, Kim H, Zhao Q. Comparative toxicokinetics of Mn chloride and methylcyclo-pentadienyl Mn tricarbonyl in male Sprague–Dawley rats. Toxicol Sci. 2000; 54:295–301. [PubMed: 10774811]

Zheng W, Zhao Q. Fe overload following Mn exposure in cultured neuronal, but not neuroglial cells. Brain Res. 2001; 897:175–9. [PubMed: 11282372]

Zheng W, Zhao Q, Slavkovich V, Aschner M, Graziano JH. Alteration of Fe homeostasis following chronic exposure to Mn in rats. Brain Res. 1999; 833:125–32. [PubMed: 10375687]

Zheng W, Ren S, Graziano JH. Manganese inhibits mitochondrial aconitase: a mechanism of Mn neurotoxicity. Brain Res. 1998; 799:334–42. [PubMed: 9675333]

Zheng W, Aschner M, Ghersi-Egea JF. Brain barrier systems: a new frontier in metal neurotoxicological research. Toxicol Appl Pharmacol. 2003; 192:1–11. [PubMed: 14554098]

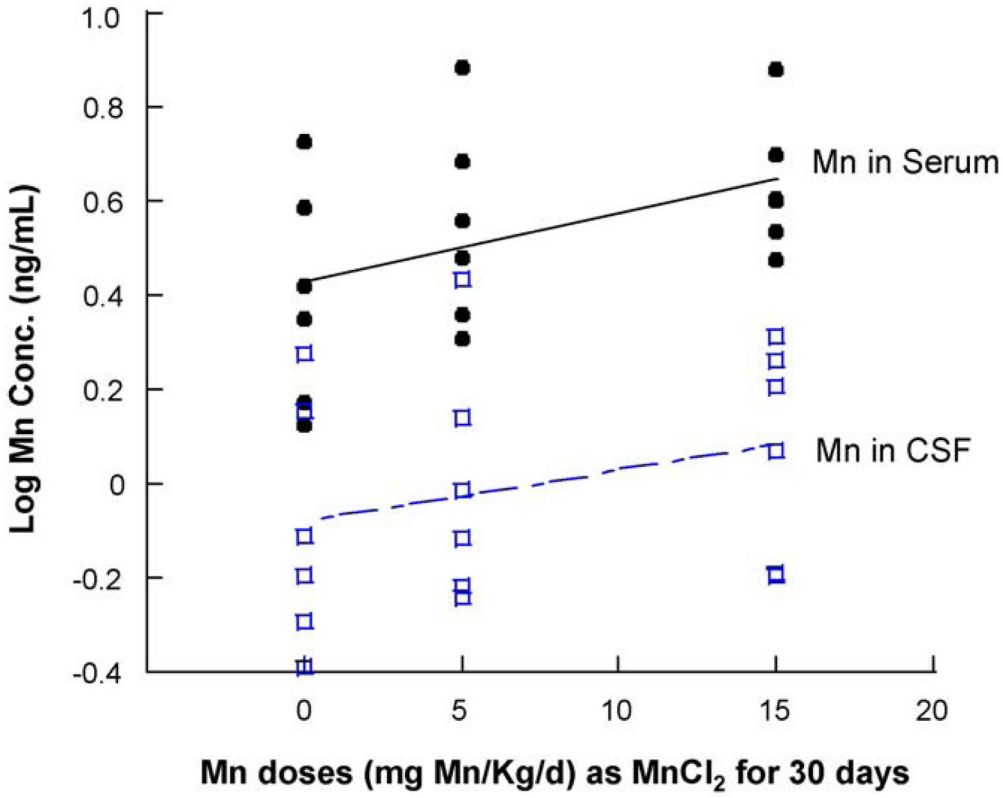

Fig. 1.

Mn concentrations in serum and CSF following subchronic Mn exposure. Rats received oral gavage of Mn at 5 or 15 mg/kg as $MnCl_2$ once daily for 30 days. Serum and CSF samples were collected and assayed for Mn by AAS. Data represent mean ± S.E.M., $n = 6$. The logarithmic regression equation for Mn in serum: $Y = 0.426 + 0.015X$, $r = 0.463$, $p = 0.030$; the equation for Mn in CSF: $Y = -0.078 + 0.011X$, $r = 0.292$, $p = 0.257$.

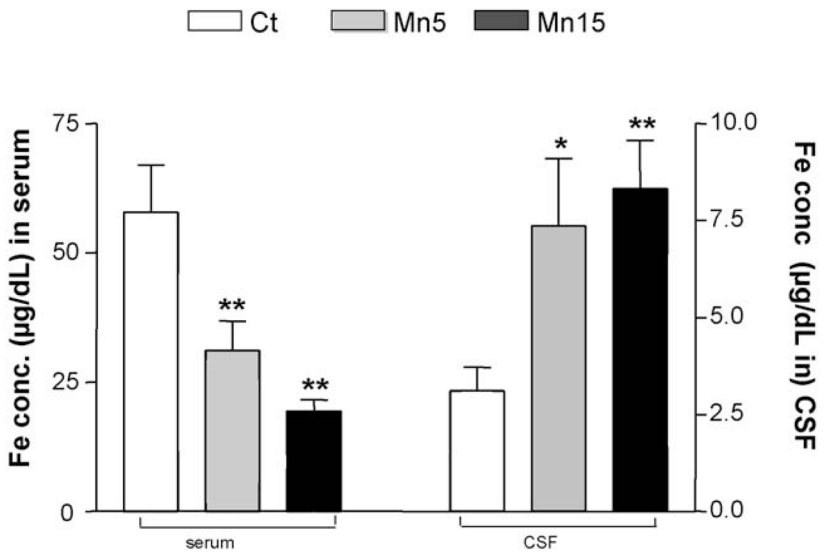

Fig. 2.

Decreased Fe concentrations in serum and increased Fe in the CSF following subchronic Mn exposure. Rats received oral gavage of Mn at 5 or 15 mg/kg as $MnCl_2$ once daily for 30 days. Serum and CSF samples were collected and assayed for Fe by AAS. Data represent mean ± S.E.M., $n = 6–11$. $^{*}p < 0.05$ as compared to controls. $^{**}p < 0.01$ as compared to controls. Ct: control group; Mn5: oral dose of 5 mg Mn/kg/day as $MnCl_2$; Mn15: oral dose of 15 mg Mn/kg/d as $MnCl_2$.

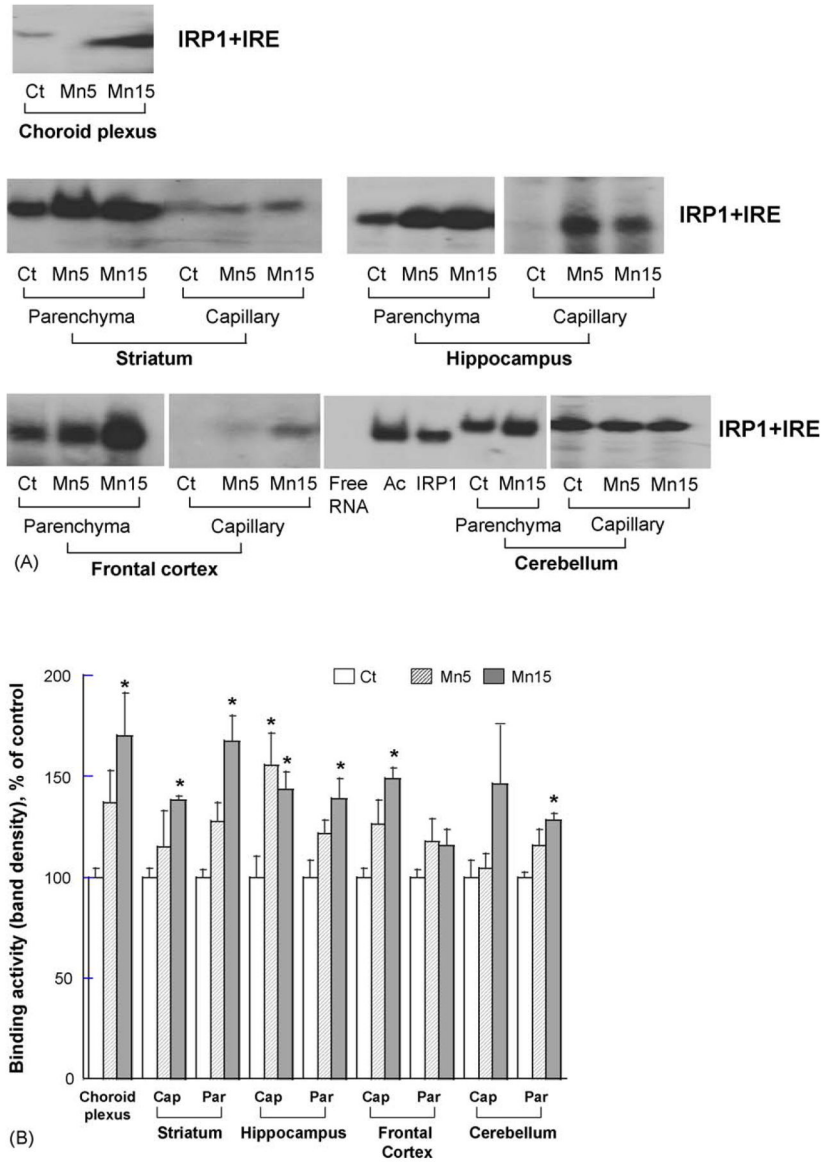

Fig. 3.

Effect of subchronic Mn exposure on the binding of IRP1 to IRE-containing RNA in the blood–CSF barrier, regional blood–brain barrier, and selected brain parenchyma by gel shift assay. S100 cytoplasmic protein extracts were incubated with ^{32}P-labeled Ft-IRE, followed by separation on non-denatured gel. (A) A representative autoradiography of three independent experiments. Ct: control group; M5: oral dose of 5 mg Mn/kg/d as $MnCl_2$; M15: oral dose of 15 mg Mn/kg/d as $MnCl_2$; Ac: aconitase from porcine as positive control; IRP1: purified IRP1 from human as positive control. (B) The band densities were quantified and expressed as Mean ± S.E.M., $n = 3$. $^{*}p < 0.05$ as compared to controls. Cap: brain endothelial capillaries; Par: brain parenchyma.

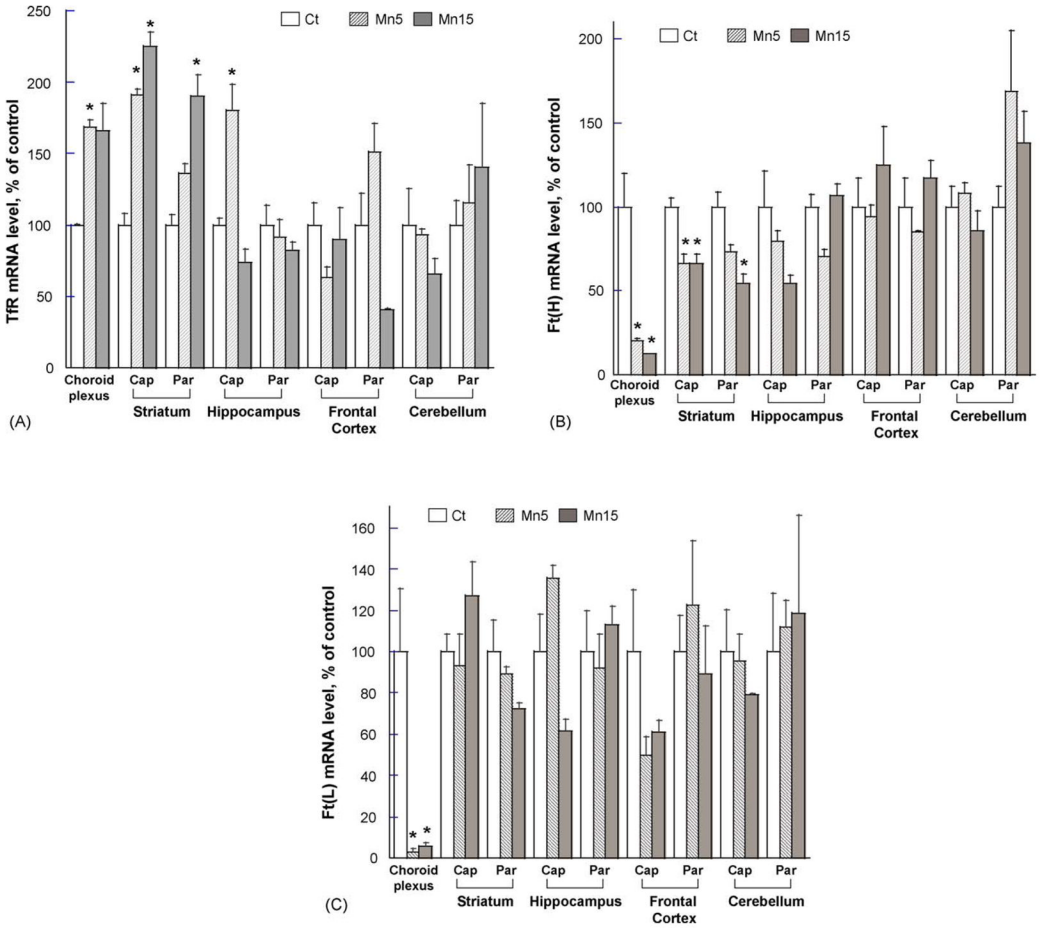

Fig. 4.

Quantitative real-time RT-PCR analyses of the expression of TfR and Ft mRNA in blood–CSF barrier, blood–brain barrier, and selected brain parenchyma following Mn exposure in rats. Total RNA was extracted from the choroid plexus, brain regional capillaries and parenchyma, followed by reverse-transcription to cDNA for amplifications. The samples were analyzed for (A) TfR, (B) Ft heavy chain, or (C) Ft light chain. Relative differences between groups were analyzed using cycle time values. The values were initially normalized by those of GAPDH in the same samples and expressed as a percentage of controls. Data represent mean ± S.E.M., $n = 3$. $^{*}p < 0.05$ as compared to controls. Ct: control group; Mn5: oral dose of 5 mg Mn/kg/d as $MnCl_2$; Mn15: oral dose of 15 mg Mn/kg/d as $MnCl_2$. Ft(H): ferritin heavy chain; Ft(L): ferritin light chain.